Low-temperature magnetic behavior of nanostructured ferrite compositions prepared by plasma spraying

A.A. Lepeshev[1,2,a)], A.V. Ushakov[1,2], I.V. Karpov[1,2]

[1] Krasnoyarsk Scientific Center of the Siberian Branch of the Russian Academy of Science, 660036, Krasnoyarsk, Russia.

[2] Siberian Federal University, Krasnoyarsk, 660041 Russia.

[a)] Author to whom correspondence should be addressed. Electronic mail: sfu-unesco@mail.ru

Abstract

Peculiarities of low-temperature behavior of the magnetic properties of disordered spinel ferrites, prepared by means of dilution with P_2O_5 amorphizing agent and by rapid quenching, were investigated. A sharp increase in the saturation magnetization σ_S, of ferrite compositions $(1-x)Me\mathrm{Fe_2O_4 \cdot xP_2O_5}$ (where Me is Ni, Fe, Mn, etc.), was observed at temperatures $T < 80$ K. It was established that the temperature dependences of σ_S and χ^{-1} (where χ is the magnetic susceptibility) of the nickel ferrite composition ($x = 0.6$) have an extremum at $T = 11$ K. In this case, the effect of "memory" is observed for $\sigma_S(T)$, which represents the dependence of σ_S ($T = 4.2$ K) on the magnitude of the magnetic field in which cooling was carried out. The asymptotic Curie temperature was determined by extrapolation of the linear part of the $\chi^{-1}(T)$ dependence, and found to be equal to -150 K. We present an analysis of the observed dependences from the point of view of a complex magnetic state, combining the features of the near antiferromagnetic and ferrimagnetic boundary-surface spin ordering.

Keywords: magnetic properties, spinel ferrites, plasma spraying.

I. INTRODUCTION

The current interest in magnetic nanosystems [1, 2] is caused not only by peculiarities of changes in the fundamental properties of nanoparticles corresponding to the decrease in size, but also by their potential applications in modern/advanced high-technology functional devices [3].

Considerable attention [4–7] has been paid to the production of magnetic glass, application of magnetic nanoparticles as additives, or use of highly concentrated paramagnetic impurities (> 30%). This glass possesses a high magnetic permeability in weak magnetic fields, and ischaracterized by transparency in the visible and near infrared bands. These characteristics permit their use in the production of new efficient magneto-optical sensors and transducers.

Another approach used to produce magnetic nanosystems includes a dilution of initial magnetic materials with amorphizing additives, for example, in the case of ferrites these are P_2O_5, B_2O_3, SiO_2, Bi_2O_3 [8–11].

As a result of these additives, both amorphous and nanostructured materials can be obtained.

X-ray amorphous materials were produced, in some cases, at high concentrations of the amorphizing agent (> 40%). The structural disorder involved in this process causes changes in the equilibrium distribution of cations on sublattices [9, 11, 18]. This leads to the frustration of exchange coupling and modification of intrasublattice and intersublattice exchange interactions, and consequently to the formation of a new magnetic state and new magnetic properties of the compositions.

It is possible to enhance the features of nanostructured ferrite compositions containing significantly less amorphizing agent, by achieving a high rate of melt cooling, for example, by means of plasma spraying, which provides a quenching rate of $10^7 - 10^8$ deg/s [11]. The potential to create such ferrite compositions are of interest for fundamental and applied sciences.

This paper presents corresponding results of studies of low-temperature magnetic behavior for nanostructured ferrite compositions $(1-x)Me\text{Fe}_2\text{O}_4 \cdot x\text{P}_2\text{O}_5$, (where Me is Ni, Fe, Mn etc.), produced by rapid quenching of molten droplets after plasma spraying.

II. EXPERIMENTAL

The preparation of $(1-x)Me\text{Fe}_2\text{O}_4 \cdot x\text{P}_2\text{O}_5$ ferrite compositions was carried out in two stages. In the first stage, the initial crystalline spinel ferrite powders $Me\text{Fe}_2\text{O}_4$, were synthesized according to the ceramic technology. In the second stage, the ferrites were sintered in air at a temperature $T = 1400$ K for four hours, followed by slow cooling. Then, after adding the required amount of phosphorus pentoxide, sintering of this mixture was carried out, at $T = 1100$ K, to prepare the ferrite compositions.

Plasma spraying of the ferrite composite powder (with a dispersion of $50 < d < 80$ µm) was carried out using a plasma arc with a coaxial input of powder into the cathode space in the $(\text{Ar} + \text{CO}_2)$ plasma medium, and a power arc discharge of 10–12 kW [11]. In some cases, in order to eliminate the dependence of the material properties on the conditions of its production, the spraying process parameters remained constant (Table 1).

Table 1 – Parameters of plasma spraying of ferrite compositions.

Power of spraying, kW	10
Arc current, A	200
Distance of sputtering, mm	120
Diameter of the nozzle, mm	5
Consumption / (flow rate) of plasma-forming gas Ar, m^3 / h	1.2
Consumption / (flow rate) of transporting gas CO_2, m^3 / h	2.2

In order to achieve high cooling rates ($V_{cooling} \sim 10^7 - 10^8$ deg/s), the spraying process was carried out on the polished surface of a rapidly rotating copper disc ($12 \cdot 10^3$ rpm).

Thus, the structural disorder and amorphization of ferrite compositions was achieved by diluting the original ferrite with the amorphizing agent (P_2O_5), followed by rapid quenching of molten droplets on a copper disk. The results of the morphological and structural studies of the produced samples are given in [11–13, 18].

The phase composition of the obtained sample was performed using Advance D8 X-ray diffractometer in CoK_α monochromatic radiation.

Images of the surfaces of ferrite compositions were obtained by means of a scanning microscope JSM-7001 F. Magnetic measurements were made with a vibrating and SQUID magnetometers. The temperature dependence of the magnetization $\sigma(T)$, was measured under two sets of conditions: cooling within a zero external field [zero field cooled (ZFC)], and after cooling within an external magnetic field [field cooled (FC)].

III. RESULTS AND ANALYSIS

After plasma spraying and rapid quenching of the drops on the copper disk, the characteristics of X-ray diffraction pattern of the ferrite compositions were substantially changed. Broadening and disappearance of sharp diffraction lines, characteristic of long-crystalline order, and emergence of clearly defined diffuse scattering, characteristic of the amorphous state were observed.

Fig. 1 shows an example of such a change in the form of an x-ray image of quenched powder compositions based on cobalt ferrite $(1-x)CoFe_2O_4 \cdot xP_2O_5$. The diffraction pattern of the samples with a low content of P_2O_5 (about 10-35%) appears as a group of broadened reflexes corresponding to a spinel structure. Since phosphorus-containing compounds are the first to become amorphous while quenching, samples are likely to have amorphocrystalline

condition. The x-ray pattern of the ferrite compositions with P_2O_5 content exceeding 35%, do not exhibit Bragg reflections, which indicates the amorphous state of the samples.

Under the fixed quenching conditions, the minimum concentration of P_2O_5 at which a transition into the amorphous state is observed, reflects propensity of ferrite compositions to become amorphous. Ferrite components from the studied composition can be arranged in order of increasing propensity to amorphisation: $Fe_3O_4 < CoFe_2O_4 < Mn-Zn < Ni - Zn < NiFe_2O_4$.
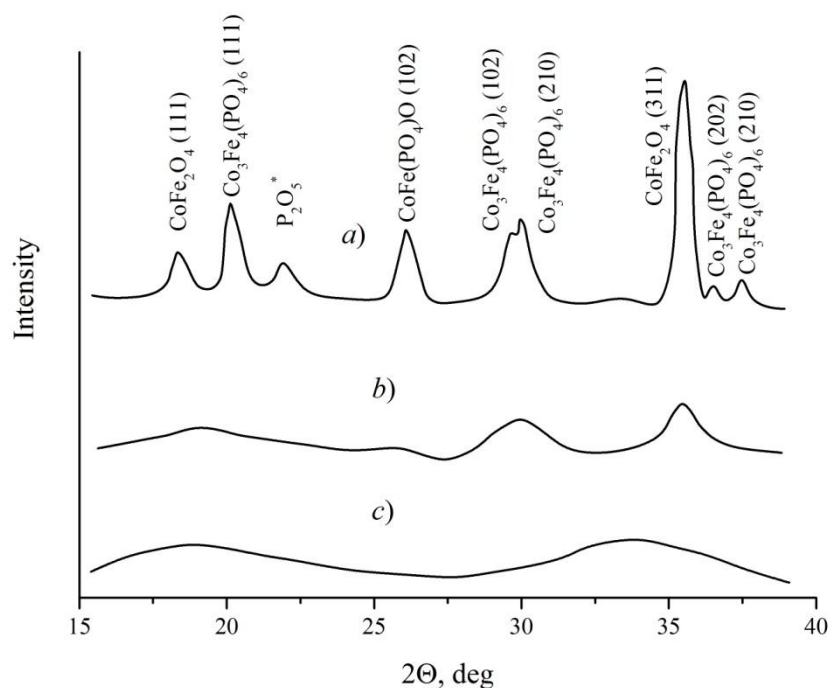

FIG. 1. X-ray of the quenched ferrite compositions $(1-x)CoFe_2O_4 \cdot xP_2O_5$.
(*a*) initial, *x*=0.35; (*b*) quenched, *x*=0.35; (*c*) quenched, *x*=0.45

The microstructure of the produced ferrite compositions appeared to be very interesting, and is shown in Fig. 2. Despite the relatively high rate of quenching ($\sim 10^7$ deg/s) and the dilution of the initial ferrite by amorphizing additives of P_2O_5, some self-organizing processes are observed in the deposited ferrite compositions. The microstructure of the quenched Ni-Zn ferrite composition (*x* = 0.4) represents an ensemble of well-ordered 200–250 nm

5

nanospheres. On closer examination, one can see that the nanospheres are heterogeneous and consist of smaller formations with size of 30–50 nm (Fig. 2c).

The conditions of slower heat transfer between the particle and the cooled base (defects, inhomogeneity, dirt in pores, etc.) leads to the formation and growth of crystal nuclei [12].

One of the particularities of the investigated ferrites ($x = 0$), regardless of their chemical composition, was a sharp decrease in the saturation magnetization σ_S, after the rapid quenching process (Fig. 3). Compared with the bulk polycrystalline ferrites, the range of σ_S change was more than 30%. It is not possible to explain this observed significant change is σ_S by non-equilibrium distribution of cations on sublattices. Evidently, rapid quenching of the melt results in the simultaneous deformation of backbone oxygen atoms and the redistribution of cations. This leads to changes in the crystal field symmetry, and in the value and type of exchange bonds under study.

As was expected, the dilution of ferrites by phosphorous pentoxide resulted in subsequent reduction of the saturation magnetization σ_S. The behavior of the temperature change in σ_S (at $T > 100$ K), and of the Curie temperature T_c, of the X-ray amorphous samples, are approximately the same as the initial ferrites.

Among the changes in the magnetic properties of the ferrite compositions, a sharp increase in magnetization at low temperatures should be mentioned in particular (Fig. 4). The described abnormal changes of σ were observed within the temperature range of 4.2–80 K, while their value depended on the sample composition.

We should also note, that such a character of the temperature change in the magnetization of ferrite (without additives of P_2O_5, when x = 0) is exhibited after rapid quenching (Fig. 4 insert). It can be assumed that this is due to the formation of nanostructured and amorphous bulky regions in the thinnest sites

(less than 0.1 μm) of quenched ferrite flakes. This is confirmed by the electron diffraction studies, while the electron diffraction patterns had an intense halo, especially along the edges of thin flakes of ferrites [11]. The results of the studies given in [19], also confirm this conclusion. Since the part of such regions in the quenched ferrites (x = 0) is not large, so the value of the temperature change in magnetization in comparison with ferrite compositions (x = 0.4) is much less.
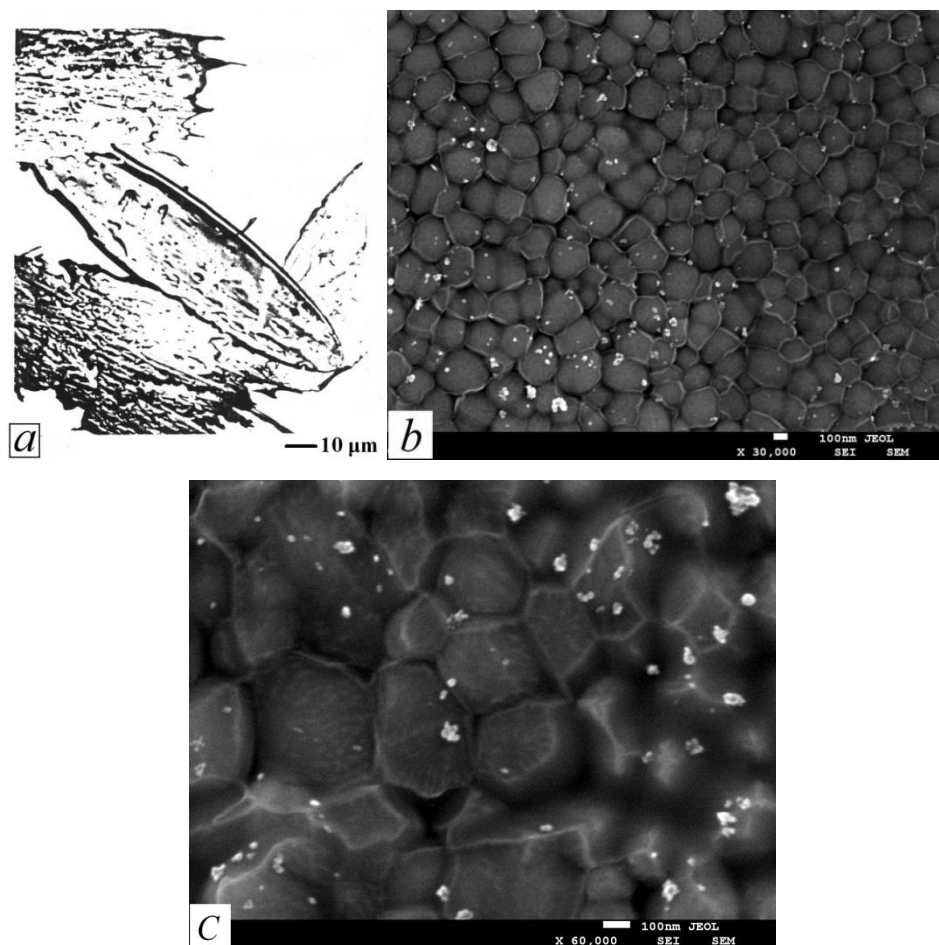

FIG. 2. The morphology of the Ni-Zn quenched particles within ferrite compositions:(*a*) form of the particles of ferrite quenched on a rotating copper disc, (*b*) shows the particle microstructure, (c) structure of nanosphere
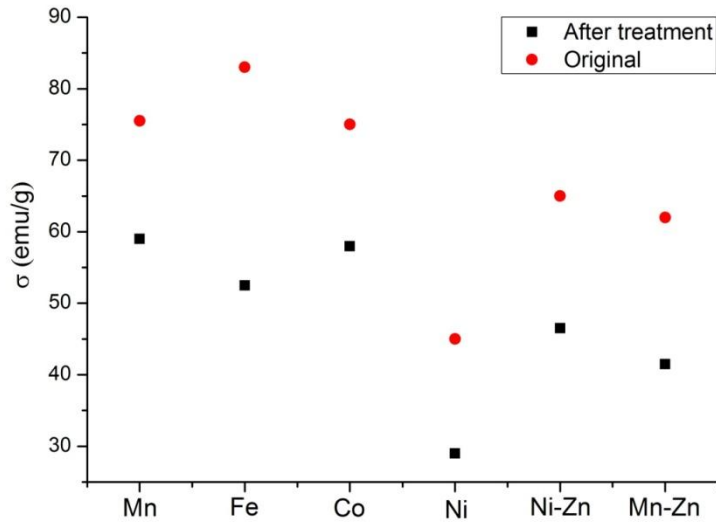
FIG. 3. Saturation magnetization of ferrites $Me\text{Fe}_2\text{O}_4$, where Me is Mn, Fe, Co, Ni, Ni-Zn, Mn-Zn. (●)– the initial ferrites, (■)– after plasma spraying and rapid quenching on the copper disk
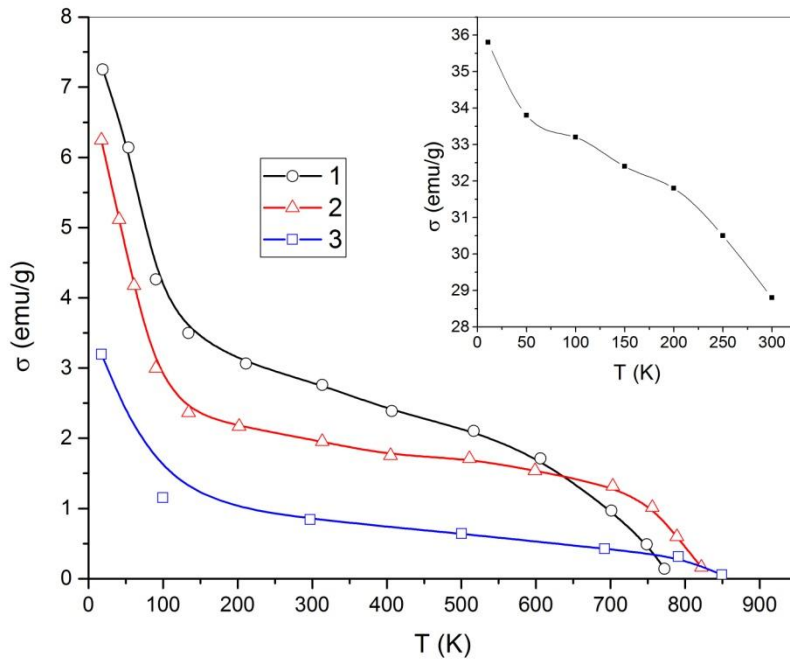

FIG. 4. The temperature dependence of magnetization for ferrite compositions 0.6 $Me\text{Fe}_2\text{O}_4$·0.4 P_2O_5: *(1)Me*-Mn; *(2) Me*-Fe; *(3) Me*-Ni. The inset: the

temperature dependence of magnetization for rapid quenched nickel ferrite

(without P_2O_5 additives, $x = 0$)

Let us consider the ferrite composition based on a well-known nickel ferrite [15]. Fig. 5 shows the temperature magnetization dependence of the nickel ferrite sample with the composition corresponding to $x = 0.6$. It is obvious that when the sample is cooled without an external magnetic field, the initial magnetization increase is followed by a decrease, corresponding to clear manifestation of the maximum at $T = 11$ K. The position of the temperature peak, and its relative value, changes depending on the percentage of P_2O_5 in the composition.

The behavior of this temperature dependence $\sigma(T)$, will be different if cooling is carried out in an applied magnetic field. In this case, at temperatures below $T = 11$ K, the difference between the magnetization values of the samples cooled in and without the magnetic field, becomes evident. This difference increases with decreasing temperature or increasing magnetic field, when the cooling process is carried out.

The behavior of $\sigma(T)$, mentioned above, is usually characteristic of a superparamagnetic state, and it is explained by the blocking temperature of magnetic moments within separate nanostructured volume formations in the corresponding material. In this case, the magnetization of an ensemble of similar superparamagnetic nanostructured volume formations can be described by the Langevin equation. The position of the blocking temperature T_b, which depends on the volume of the particles and their anisotropy, can be described by the equation $T_b = KV/25k_B$. Here, K is an anisotropy component, V is the volume of a nanostructured volume formation, and k_B is the Boltzmann constant.

Let us use this ratio to estimate the effective magnetic anisotropy constant for nanostructured volume formations of a ferrite composition based on nickel. Assuming that the blocking temperature is equal to $T_b = 11$ K (Fig. 4), and that

the size of the nanostructured volume formation is $d = 30$ nm, we obtain a value for the effective magnetic anisotropy constant, $K_{eff} = 0.27 \cdot 10^4$ erg/cm^3. This value is more than an order of magnitude smaller than the constant of bulk nickel ferrite, which isequal to $K = 6.2 \cdot 10^4$ erg/cm^3 [15, 16].

Such a large discrepancy in the magnitudes of the magnetic anisotropy constant is probably due to the presence of other mechanisms in its formation, or due to a much smaller size of the nanoparticles (< 5 nm). In favor of the latter assumption, the data of γ-resonance spectroscopy (γ-spectra is modified into a doublet) indicate the absence of long-spin ordering in nickel ferrite compositions (at $x > 4$) [18]. In this case, the magnetic structure represents clusters formed by the near magnetic order.

In such nanosized regions, the ratio of magnetoactive ions inside the region and at its boundary becomes equal, and the role of boundary-surface spins in the formation of magnetic properties increases significantly. As a result of the change in the structure and exchange bonds, the boundary-surface spins become disordered and are not oriented along the direction of local anisotropy, which can lead to a significant increase in anisotropy in comparison with the nano-region center [20].

Apparently, this is a reason of unsaturability of the magnetization curves of the investigated ferrite compositions even in high magnetic fields (up to 50 kOe).
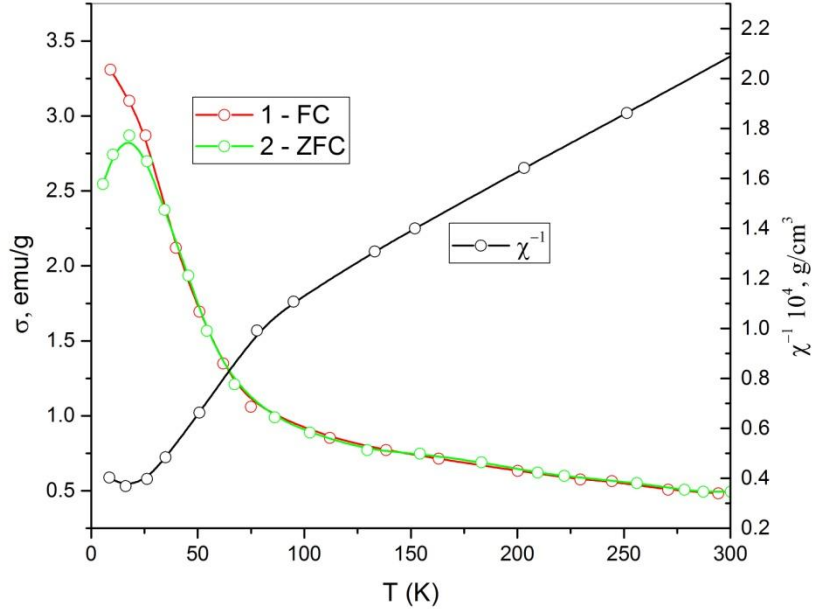
FIG. 5. The temperature dependence of the magnetization σ and the susceptibility χ for the composition of $0.4NiFe_2O_4\cdot0.6P_2O_5$: (*1*) is cooled in the field of 1.06 kOe (FC); (*2*) is zero field cooled (ZFC).

Fig. 5 also shows the temperature dependence of the inverse susceptibility, which characterizes the behavior of the magnetization in high fields. At temperatures greater than 80 K, the inverse susceptibility $\chi^{-1}(T)$, is well described by the Curie-Weiss law. At low temperatures, a noticeable deviation of $\chi^{-1}(T)$ from a linear dependence, and the appearance of the minimum at $T = 11$ K, are observed. The extrapolation of the linear portion of the $\chi^{-1}(T)$ data to a cross-section with the X-axis gives the value of the asymptotic Curie temperature, $T_c \sim -150$ K. This indicates the appearance of strong antiferromagnetic correlations at $T \sim 11$ K.

We should note that, in this case, antiferromagnetism should not be classically understood as a set of magnetic sublattices compensating each other. This is only about a short-range antiferromagnetic order, that is, antiferromagnetic correlations propagating, apparently, within several coordination spheres.

11

The peculiarities of magnetization of ferrite compositions are represented by the example of $0.4NiFe_2O_4 \cdot 0.6P_2O_5$ (Fig. 6). The rapid increase in magnetization in weak magnetic fields and a subsequent nearly linear increase, which depends on the external field, are observed at T=300 K. The discussed increase of $\sigma(H)$, without evidence of saturation, was observed for fields of up to 50 kOe. While cooling of the sample is provided in the magnetic field, the unidirectional magnetic anisotropy appeared; the magnetization curves shifted along the X-axis in the direction opposite to the applied field.
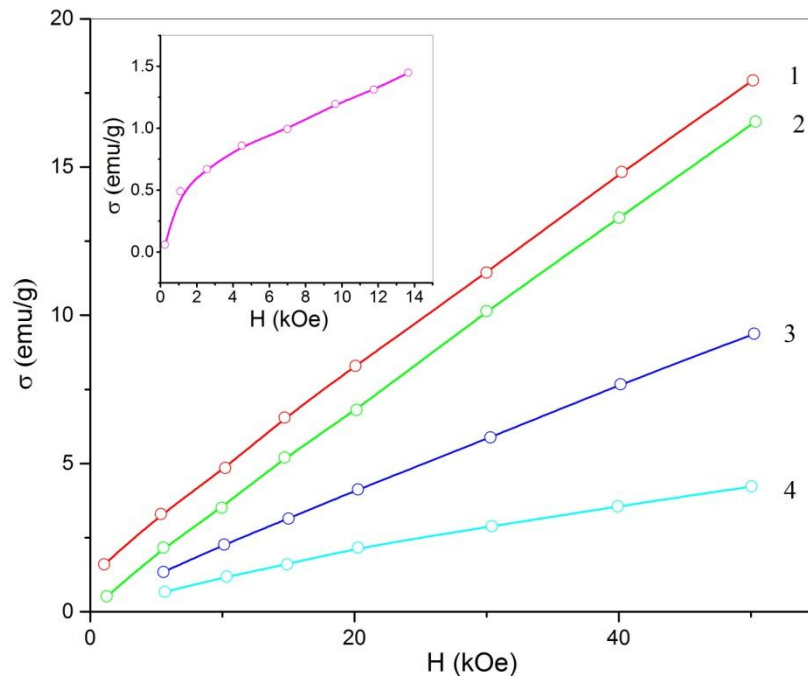

FIG. 6. The magnetization curves for the sample of $0.4NiFe_2O_4 \cdot 0.6P_2O_5$:(*1*) is of 4.2 K and 10.55 kOe field cooled (FC); (*2*) is of 4.2 K zero field cooled (ZFC); (*3*) is of 77 K; (*4*) is of 300 K (The inset shows the initial part of the magnetization curve at $T = 300$ K).

The described complexity of the magnetic properties of the ferrite compositions is typical for a class of magnetic materials called mictomagnets [17]. These materials do not demonstrate long-spin ordering at low temperatures. Instead, they show a specific magnetic state characterized by

frozen spin directions and a combination of different types of exchange interactions.

Based on the experimental data analysis, the observed change in the magnetic state of ferrite compositions under lower temperatures can be assumed as follows. The rapid quenching process, and the dilution of the initial ferrite with phosphorus pentoxide, results in the formation of structural-disordered nanostructured volume formations.

In these nanostructured volume formations, definite exchange fluctuations and frustration of negative exchange couplings occur, but spin ordering (ferrimagnetic, antiferrimagnetic) remains unchanged. This assumption is based on the preservation that we observe of the properties of the initial ferrites under study: the identical behavior of the temperature-based magnetization change at $T > 100$ K, and a slight shift of the Curie temperature, asymptotic Curie temperature.

Cooling the sample down to liquid-helium temperatures, apparently, causes fixation of boundary surface-spins in X-ray amorphous ferrite compositions. It causes the appearance of the fields of anisotropy,which block the thermal motion of the magnetic moments. In that case, when the cooling process is performed in a magnetic field, and long before the moment when the blocking temperature is reached, we observe that the magnetic moments of the nanostructured volume formations are mostly aligned with the field, and are fixed in this state on passing through the blocking temperature.

IV. CONCLUSION

It was revealed that, under cooling, a complex magnetic state is observed in X-ray amorphous ferrite compositions $(1-x) \cdot Me\mathrm{Fe_2O_4} \cdot x\mathrm{P_2O_5}$ (where Me is Ni, Fe, Mn, etc.). This state combines features of short-range ferrimagnetic ordering and antiferromagnetic correlations. The observed set of magnetic properties

corresponds to this state. They are: a sharp increase in the magnetization σ of ferrite compositions at temperatures $T < 80$ K; the presence of an extremum in the temperature dependences of σ and χ^{-1} (χ is a magnetic susceptibility) of the nickel ferrite composition ($x = 0.6$) at $T = 11$ K; the effect of "memory", which represents the dependence of σ ($T = 4.2$ K) on the magnitude of the magnetic field in which cooling was carried out; a rapid increase in the magnetization of the nickel ferrite composition in weak magnetic fields (~ 1 kOe) and an almost linear further increase in the fields up to 50 kOe; the presence of the asymptotic Curie temperature in the nickel ferrite composition ($x = 0.6$) found to be equal to - 150 K.

References

1. A.V. Ushakov, I.V. Karpov, A.A. Lepeshev, L.Yu. Fedorov, A.A. Shaikhadinov, *Technical Physics* **61**, 103 (2016).

2. A.V. Ushakov, I.V. Karpov, A.A. Lepeshev, M.I. Petrov, L.Yu. Fedorov, *Physics of the Solid State* **57**, 919 (2015).

3. M. Sugimoto. *J. of the American Ceramic Society* **82**, 269 (1999).

4. N. Rezlescu, L. Rezlescu. *Materials Science and Engineering: A* **375-377**, 1273 (2004).

5. H. Akamatsu, K. Tanaka, K. Fujita, S. Murai. *Journal of Physics: Condensed Matter.* **20**, 235216 (2008).

6. K. Sharma, Sher Singh, C.L. Prajapat, S. Bhattacharya, Jagannath, M.R. Singh, S.M. Yusuf, G.P. Kothiyal. *Journal of Magnetism and Magnetic Materials*. **321**, 3821 (2009).

7. R.P. Maiti, S. Basu, S. Bhattacharya, D. Chakravorty. *Journal of Non-Crystalline Solids* **355**, 2254 (2009).

8. M. Fahmy, M. Park, M. Towasara, R.K. Mac Crone. *Physics and Chemistry of Glasses* **13**, 21 (1972).

9. M. Sugimoto, N. Hiratsuka. *JMMM*. **3**, 1533 (1983).

10. M. Sugimoto. *JMMM* **133**, 460 (1994).

11. A. Lepeshev. Amorphous and nanocrystalline materials of plasma spraying. Lambert Academic Publishing. 2015. 308 p.

12. A.A. Lepeshev, I.V. Karpov, A.V. Ushakov, G.E. Nagibin. *Journal of Alloys and Compound*s **663**, 631 (2016).

13. A.V. Ushakov, I.V. Karpov, A.A. Lepeshev, M.I. Petrov. *Vacuum* **133**, 25 (2016).

14. A.V. Ushakov, I.V. Karpov, A.A. Lepeshev, L.Yu. Fedorov, A.A. Shaikhadinov. *Technical Physics* **86**, 103 (2016).

15. Y. Smit, Kh. Wein. Ferrites. Moscow, 1964.

16. A.V. Ushakov, I.V. Karpov, A.A. Lepeshev. *Journal of Superconductivity and Novel Magnetism* **30**, 311 (2017).

17. S. Tikadzumi. Physics of Ferromagnetism. Moscow, 1983. 304 p.

18. Lepeshev A.A., Karpov I.V., Ushakov A.V., Nagibin G.E. Magnetic and resonant properties of ferrite compositions $(1-x) \cdot Me\text{Fe}_2\text{O}_4 \cdot x\text{P}_2\text{O}_5$ prepared by plasma spraying. *Mater. Res. Express* **4** (2017) 056101.

19. Maaz K., Mumtaz A., Hasanian S.K., Bertino M.F. Temperatute dependent coercivity and magnetization of nickel ferrite nanoparticles. *J. Magnetism and Magnetic Materials*. **322** (2010), 2199-2202.

20. Kodama R.H., Berkowitz A.E. *J. Appl. Phys.* **81** (8), 1997, 5552-5557.